AJNR

This information is current as of August 14, 2025.

Technical factors of CT angiography studied with a carotid artery phantom.

S W Wise, K D Hopper, T A Schwartz, T R Ten Have and C J Kasales

AJNR Am J Neuroradiol 1997, 18 (3) 401-408
http://www.ajnr.org/content/18/3/401

Technical Factors of CT Angiography Studied with a Carotid Artery Phantom

Scott W. Wise, Kenneth D. Hopper, Todd A. Schwartz, Thomas R. Ten Have, and Claudia J. Kasales

PURPOSE: To evaluate scanning parameters (conventional versus spiral CT, section thickness, and pitch) and vessel orientation in the performance of CT angiography. **METHODS:** Conventional CT and 1.0-, 1.5-, and 2.0-pitch spiral CT acquisitions of a carotid phantom designed with vessels oriented parallel to the z-axis, 45° oblique, and perpendicular to the z-axis were obtained with section thicknesses of 2, 4, and 8 mm. The phantom contained 32 vessels with 0% to 100% stenoses. Normal and stenotic luminal diameters were measured and the number of artifacts was assessed. **RESULTS:** No overall difference was observed among conventional and spiral CT acquisitions obtained with pitches of 1.0, 1.5, and 2.0. With thicker sections, CT angiographic accuracy decreased and artifacts increased. The three-vessel orientations were relatively comparable in accuracy in terms of the percentage of stenosis measured. Vessels parallel to the z-axis suffered less artifactual degradation. Unique artifacts, such as luminal distortion and beam hardening, were observed in vessels oriented at 45° and perpendicular to the z-axis. **CONCLUSION:** Use of thinner sections with vessels oriented parallel to the z-axis optimizes CT angiographic quality. There is no apparent degradation with the use of spiral CT, and a pitch of 1.5 or 2.0 provides results equivalent to 1.0-pitch spiral studies.

Index terms: Arteries, computed tomography; Arteries, stenosis and occlusion; Computed tomography, three-dimensional

AJNR Am J Neuroradiol 18:401–408, March 1997

The advent of spiral (helical) computed tomography (CT) has created a potential role for CT angiography in clinical applications. The speed of current scanners enables dynamic imaging during peak bolus intravenous contrast enhancement. As a result, CT angiographic protocols can be tailored to maximize luminal enhancement of the blood vessels that are of specific clinical interest. In addition, spiral imaging minimizes motion artifacts, allows a large volume to be imaged during a single breathhold with thinner sections, and eliminates section-to-section misregistration. New contrast timing sequences, such as SVIP (Picker International, Highland Heights, Ohio) and Smart Prep (General Electric Medical Systems, Milwaukee, Wis) further increase the quality of CT angiography by allowing more accurate timing of the contrast bolus. Additionally, present-day computers have made the use of multiplanar and three-dimensional reconstructions easier, faster, and more practical for clinical applications (1).

The use of CT angiography has been investigated in the study of a multitude of blood vessels throughout the body (2–5). These studies show CT angiography to have promise for a variety of clinical applications. Specific technical factors of CT angiography, such as the effect of section thickness and vessel orientation, have been studied (6, 7)(C. Diederichs, D. Keating, J. Oestmann, "Influence of Collimation and Threshold on Transversely Oriented Vessels in Spiral CT Angiography," *Radiology*

Received July 1, 1996; accepted after revision September 17.

Presented at the annual meeting of the Radiological Society of North America, Chicago, Ill, November 1995.

Supported by a grant from Picker International, Highland Heights, Ohio.

From the Department of Radiology (S.W.W., K,.D.H., C.J.K.) and the Center of Biostatistics and Epidemiology (T.A.S., T.R.TH.), Penn State University College of Medicine, Hershey.

Address reprint requests to Scott W. Wise, MD, Department of Radiology, Penn State University College of Medicine, 500 University Drive, Hershey, PA 17033.

AJNR 18:401–408, Mar 1997 0195-6108/97/1803–0401

© American Society of Neuroradiology

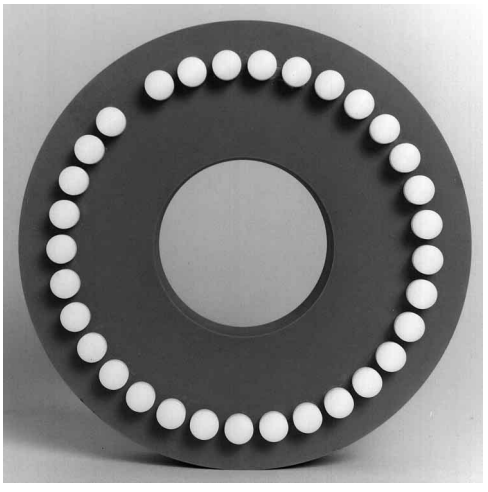

Fig 1. Frontal photograph of the Penn State CT angiographic phantom. The phantom is viewed from the outside in the same position as the CT scans in Figure 3 and the MPR images in Figure 4. The vessels are sealed with plastic plugs.

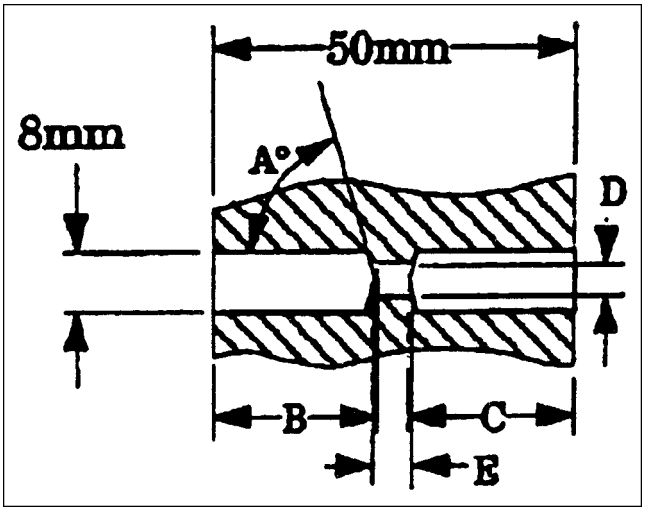

Fig 2. Diagram of a longitudinal section through a phantom vessel. Angle *A* indicates the angle of inclination into the stenoses and had a value of either 75° or 45°.

1994;193(P):171, abstract). In this study, we used a carotid phantom to assess the quality of conventional and spiral CT acquisitions obtained with pitches of 1.0, 1.5, and 2.0 in the assessment of stenoses of varying severity (0% to 100%), length, and angle of orientation relative to the z-axis.

Materials and Methods

A dedicated carotid phantom was designed for our study. The phantom was constructed of a rubber polymer of soft-tissue density (Rando, The Phantom Laboratory, Salem, NY) and contained 32 straight holes situated along the periphery (Fig 1). The holes represented vessels and had an internal luminal diameter of 8 mm.

Each vessel contained a stenosis of 0%, 50%, 75%, 94%, or 100% at its center, drilled to a hundredth of a millimeter accuracy and verified to 1 μm. Three lengths of stenoses were studied (1, 3, and 5 mm) as well as two angles of inclination into the stenosis (45° and 75°) (Fig 2). The vessels were filled with an appropriate mixture of nonionic contrast material and water to obtain a CT density of 240 Hounsfield units, which, on the basis of clinical experience, is considered to be an optimal luminal enhancement. The vessel ends were sealed with plastic plugs, which prevented the introduction of air.

The phantom was scanned (PQ 5000, Picker International, Highland Heights, Ohio) a total of 36 times in the assessment of multiple primary scanning parameters, including conventional and 1.0-, 1.5-, and 2.0-pitch spiral CT acquisitions, each obtained with section thicknesses of 2, 4, and 8 mm and at three different vessel orientations (parallel to the z-axis, 45° oblique, and perpendicular to the z-axis). Parameters of 300 mA and 120 kV were used, with a rotation of 1 second per tube. *Reconstruction interval* refers to the measurement in millimeters between image sections. The images may be contiguous, have an intersection gap, or overlap in coverage. *Section overlap* refers to the percentage of common coverage of one image with the preceding image. For this study, an appropriate reconstruction interval was used to obtain a 75% section overlap with the 4-mm and 8-mm spiral scans. A 75% overlap was not possible with the 2-mm sections and a 50% overlap was used instead. A 15-cm field of view was used for all scans and the phantom was always placed at gantry isocenter. All studies were photographed with identical window and level settings (300 and 40, respectively), chosen to provide relatively accurate measurements of luminal diameter while maintaining visible periluminal blooming or halo artifact. Although this setting has less contrast than a nominal scale, a compromise was necessary to allow simultaneous measurement of stenosis and assessment of artifact.

The luminal diameters were measured in and out of the stenoses for all 32 vessels in each of the 36 scans. A total of 5056 luminal measurements were obtained by the same blinded investigator using a dedicated computer workstation (Voxel Q, Picker International, Highland Heights, Ohio), with measurements made to within 0.1 mm. Since the imaged lumens were eccentric in the 45° oblique orientation and in the vessel orientation perpendicular to the z-axis, orthogonal measurements for these orientations were made of the long and short diameters in and out of the stenoses. As artifacts predominated along the long axis, the short diameters were subsequently used to determine the percentage of stenosis for these two orientations.

The direct CT scans were used for measurements when the vessel orientation was parallel to the z-axis. Images obtained with phantom orientations at 45° and perpendicular to the z-axis were initially reconstructed into an image parallel to the z-axis plane by using oblique multiplanar

TABLE 1: Measured percentage of stenosis relative to standard of reference by scanning technique*

Type of Scanning Technique	Actual Measurement, mm					Overall Difference from Standard of Reference
	6	4	2	1	0.5	
	Percentage of Stenosis					
	25.0	50.0	75.0	87.5	94.0	
	All Vessels					
Conventional	13.9% (1.1)	27.9% (1.9)	46.2% (2.4)	56.5% (2.6)	59.8% (2.8)	2.2
Spiral 1.0	13.8% (1.0)	29.1% (1.7)	50.3% (2.1)	59.0% (2.4)	65.8% (2.3)	1.9
Spiral 1.5	17.6% (0.7)	28.8% (1.8)	49.4% (2.1)	62.8% (2.1)	65.2% (2.4)	1.8
Spiral 2.0	9.8% (1.1)	22.3% (2.1)	44.2% (2.5)	52.3% (2.8)	56.7% (2.9)	2.3
	5-mm Long Stenoses/All Section Thickness					
Conventional	21.6% (0.5)	44.1% (0.6)	69.8% (0.5)	86.4% (0.1)	91.2% (0.2)	0.4
Spiral 1.0	21.9% (0.4)	44.1% (0.5)	73.7% (0.2)	85.8% (0.2)	94.6% (−0.0)	0.2
Spiral 1.5	28.9% (−0.2)	43.9% (0.6)	71.9% (0.3)	84.9% (0.3)	91.3% (0.3)	0.2
Spiral 2.0	17.9% (0.4)	39.8% (0.8)	72.3% (0.3)	84.0% (0.3)	85.1% (0.7)	0.5
	5-mm Long Stenoses/2-mm Section Thickness					
Conventional	23.1% (0.4)	46.7% (0.4)	74.1% (0.2)	89.7% (−0.1)	97.3% (−0.3)	0.1
Spiral 1.0	23.0% (0.4)	42.7% (0.6)	74.8% (0.1)	85.5% (0.2)	98.0% (−0.3)	0.2
Spiral 1.5	25.9% (0.2)	48.7% (0.3)	75.5% (0.1)	89.8% (−0.1)	98.0% (−0.3)	0.0
Spiral 2.0	23.8% (0.3)	43.8% (0.7)	75.2% (0.0)	88.6% (−0.0)	92.0% (0.1)	0.2

* More complete tables with 95% confidence intervals upon request.

Note.—Numbers in parentheses are the difference between the measured luminal diameter and the standard of reference.

reconstruction (MPR). Hence, all measurements could be made in the same manner using a cross section.

The extent of halo artifact and edge definition was assessed subjectively by using a quantitative five-point scale, in which a score of one indicates no artifact and a score of five severe artifact. *Edge definition* refers to the sharpness of the luminal margins; *halo artifact* refers to an increased amount of extraluminal attenuation or blooming of the vessel lumen. All artifact assessments were made by the same blinded investigator to avoid interobserver variability.

The edge definition of the vessels was graded according to the following criteria: 1) very sharp edges throughout; 2) minimal edge blur (≤ 5% of the width of the luminal diameter); 3) mild edge blur (5% to 10% of the luminal diameter, has minimal effect on luminal measurements); 4) moderate edge blur (10% to 20% of the luminal diameter, hinders accurate measurements); 5) serious edge blur (>20% of the luminal diameter, makes measurement difficult).

Halo artifact (periluminal blooming) was established with the following criteria: 1) no halo; 2) minimal halo around edges, ≤10% width of the luminal diameter; 3) mild halo (halo thickness 10% to 30% of the luminal diameter, has minimal effect on measurements); 4) significant halo (halo thickness 30% to 50% of the luminal diameter, hinders accurate measurements); 5) serious and bright halo (halo thickness ≥50% of the luminal diameter, makes measurement difficult).

Statistical analyses included multiway analyses of variance to assess interaction and make pairwise comparisons among various combinations of factors. All *P* values were derived from F-statistics obtained under the analysis of variance models and pairwise comparisons. Percentage of stenosis was calculated from measurements of the luminal diameter and compared with the standard of reference for percentage of stenosis (actual percentage of stenosis of each phantom vessel based on luminal diameters in and out of the stenosis verified to 0.01 mm by the phantom manufacturer). In addition, a direct comparison was made between the measured lumen and the standard of reference both in and out of the stenosis. Statistical analysis was performed in a similar manner to obtain scores for edge sharpness and halo artifact.

Results

Random statistical differences were noted among the techniques of conventional CT and three pitches of spiral CT. The random nature of these differences was attributed to imprecision in the luminal diameter measurements, as no significant trends were identified. The consolidated data suggest equivalency of the four scanning techniques, since there were random combinations of other factors (ie, section thickness, vessel orientation, and so on), which produced the statistically significant differences (Table 1).

No significant trends were identified in assessments of the normal-caliber (8-mm) vessel by imaging with 2-, 4-, and 8-mm section thick-

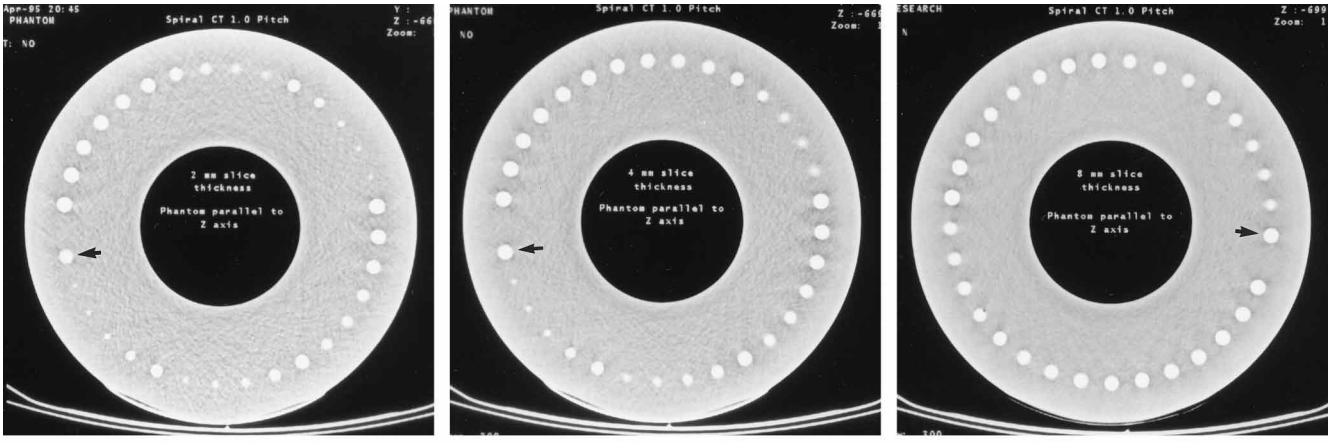

Fig 3. Spiral CT scans of the stenoses at a 1.0 pitch with the phantom vessels parallel to the z-axis. The scans are of 2- (*A*), 4- (*B*), and 8-mm (*C*) section thickness, respectively. Note the apparent increase in artifacts with thicker sections. *Arrow* points to vessel 1.

TABLE 2: Difference* in measured percentage of stenoses and luminal diameters from standard of reference by section thickness and stenosis length†

Thickness, mm	All Stenoses	1-mm Length	3-mm Length	5-mm Length
2	−19.2% (1.7)	−41.6% (3.6)	−15.5% (1.4)	−0.4% (0.1)
4	−21.9% (1.9)	−43.3% (3.6)	−21.8% (1.8)	−0.5% (0.1)
8	−33.0% (2.5)	−51.2% (3.9)	−38.0% (2.9)	−9.9% (0.8)

* Percentage of difference from standard of reference, measured minus actual (difference, mm, from standard of reference).

† More complete tables with 95% confidence intervals upon request.

nesses. However, in imaging stenoses, higher accuracy was observed with thinner sections (Fig 3). This trend was most evident with the 3- and 5-mm stenosis lengths and less obvious with the 1-mm stenosis length (Table 2). Additionally, the relative accuracy of scans with all three section thicknesses improved with increasing stenosis length ($P < .0001$).

All three vessel orientations yielded relatively accurate assessment of the percentage of stenosis. However, two trends were observed. First, the overall measurements of vessels oriented at 45° obliquity were the least accurate for estimates of stenosis. Second, the vessel orientation perpendicular to the z-axis was the most accurate (Table 3).

A direct relationship was noted between halo and edge artifacts. For example, a significant amount of halo or edge artifact was always accompanied by a similar degree of the other artifact. Additionally, halo artifacts and lack of edge definition were significantly greater in scans of stenotic vessels as compared with scans of normal-caliber vessels ($P < .0001$) (Table 4).

Significant trends were identified in regard to the degree of artifacts seen within stenoses. The 2- and 4-mm section thicknesses consistently produced better edge definition relative to the 8-mm section thicknesses ($P = .0007$). A sequential increase in halo artifacts was also observed with 2-, 4-, and 8-mm section thicknesses, respectively ($P < .0001$). Halo artifacts and loss of edge definition increased significantly with vessel orientations not parallel to the z-axis ($P < .0001$), the greatest number of artifacts observed in vessels oriented perpendicular to the z-axis (Fig 4). Overall, a similar degree of artifact was observed on both the conventional and spiral CT scans.

When the phantom vessels were oriented perpendicular to the z-axis, beam-hardening artifacts were frequently observed across the stenoses (Fig 5).These artifacts generally had little effect on measurements of mild stenoses. High-grade stenoses, however, often appeared to be completely occluded on MPR images when the beam-hardening artifact was present, leading to twice the number of false-positive findings of high-grade stenosis when vessels were oriented in the perpendicular orientation versus the 45° orientation ($P < .0001$). There were no false-

TABLE 3: Measured percentage of stenosis and luminal diameters relative to standard of reference by vessel orientation*

Vessel Orientation	Actual Measurement, mm					Overall Difference from Standard of Reference
	6	4	2	1	0.5	
	Percentage of Stenosis					
	25.0	50.0	75.0	87.5	94.0	
	All Vessels					
Parallel to Z-axis	11.9% (1.5)	23.4% (2.5)	41.5% (3.0)	51.2% (3.1)	55.1% (3.3)	2.7
45° Oblique	9.1% (1.4)	20.2% (2.4)	39.2% (2.9)	48.6% (3.2)	53.6% (3.3)	2.6
xy	20.4% (0.0)	37.4% (0.7)	61.9% (0.9)	73.1% (1.1)	76.9% (1.3)	0.8
	5-mm Stenoses/All Section Thickness					
Parallel to Z-axis	18.2% (1.0)	35.2% (1.5)	60.2% (1.4)	72.7% (1.3)	78.1% (1.3)	1.3
45° Oblique	17.4% (0.7)	41.2% (0.8)	77.0% (−0.1)	89.7% (−0.1)	96.6% (−0.2)	0.2
xy	32.2% (−0.8)	52.5% (−0.4)	78.5% (−0.3)	93.4% (−0.5)	97.0% (−0.3)	−0.5
	5-mm Stenoses/2-mm Section Thickness					
Parallel to Z-axis	23.6% (0.4)	44.0% (0.7)	74.4% (0.1)	88.2% (−0.0)	95.6% (−0.2)	0.2
45° Oblique	20.4% (0.7)	43.3% (0.8)	74.3% (0.2)	88.9% (−0.1)	98.0% (−0.3)	0.3
xy	27.8% (−0.1)	49.1% (0.0)	76.0% (−0.1)	88.1% (−0.0)	95.3% (−0.1)	−0.1

* More complete tables with 95% confidence intervals upon request.

TABLE 4: Edge and halo artifacts by scan technique, vessel orientation, and section thickness (SD)

	Edge		Halo	
	In	Out	In	Out
Technique				
Conventional	2.9 (1.1)	1.9 (0.9)	3.4 (1.2)	2.5 (1.2)
1.0 pitch	3.2 (1.2)	2.3 (1.2)	3.4 (1.3)	2.5 (1.2)
1.5 pitch	3.2 (1.3)	2.3 (1.3)	3.6 (1.3)	2.5 (1.3)
2.0 pitch	3.1 (1.2)	2.0 (0.8)	3.5 (1.2)	2.4 (1.1)
Vessel orientation				
Parallel to Z-axis	2.5 (1.1)	1.2(0.4)	2.9 (1.2)	1.4 (0.5)
45° Oblique to Z-axis	2.8 (1.0)	2.1(0.6)	3.3 (1.3)	2.5 (1.1)
Perpendicular to Z-axis	4.1 (0.9)	3.3 (0.7)	4.3 (0.8)	3.6 (0.9)
Section thickness, mm				
2	3.0 (1.1)	1.8 (0.8)	3.1 (1.2)	1.9 (0.8)
4	3.0 (1.3)	2.2 (1.0)	3.6 (1.2)	2.6 (1.3)
8	3.3 (1.2)	2.5 (1.2)	3.7 (1.3)	3.0 (1.3)

Note.—In indicates within the stenosis; out, outside the stenosis.

positive findings of occlusion when the vessels were oriented parallel to the z-axis (Table 5).

An additional artifact involving distortion of luminal shape was observed with the 45° oblique orientation and the orientation perpendicular to the z-axis. The MPR images of vessels scanned in these orientations showed an eccentric or oval appearance of the lumen. For both vessel orientations, the degree of eccentricity (as measured by a short-to-long axis ratio) was significantly greater on images of the stenoses than on images of the normal lumen ($P < .0001$). Halo and edge artifacts appeared to be preferentially distributed along the long axis when this luminal distortion was present.

Discussion

Several previous studies have evaluated the clinical application of CT angiography in the assessment of carotid arteries. The overall agreement in these studies between CT angiography and conventional carotid arteriography ranged from 50% to 98% (2, 8, 9), and the correlation between CT angiography and carotid duplex and magnetic resonance (MR) angiography ranged from 90% to 98% (2). These results reflect the potential of CT angiography in the evaluation of carotid disease.

We designed our phantom in the model of a carotid artery because of the relatively straight course of most carotid arteries and the prevalence of carotid disease. Although the 45° oblique vessel orientation and the orientation perpendicular to the z-axis are seen infrequently in carotid CT angiography, they are encountered at the bifurcation and in tortuous or looped carotid arteries.

Although there was some random variability in our data, we did not identify any significant overall differences among conventional CT and the three pitches of spiral CT. However, the single most advantageous aspect of spiral CT is

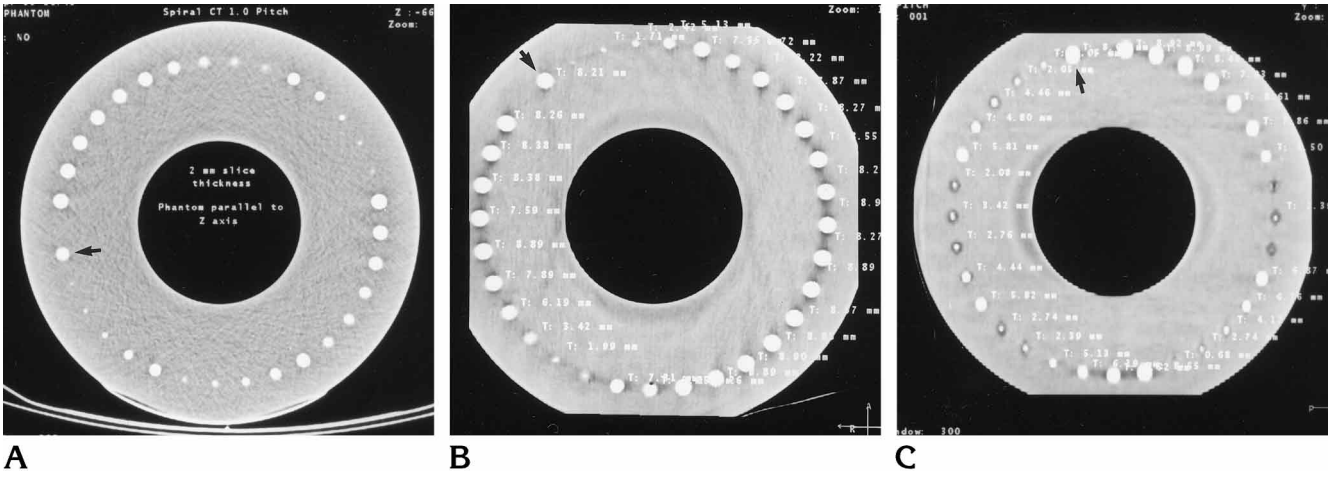

Fig 4. Scans obtained through the stenoses with the phantom vessels parallel (*A*), at a 45° oblique orientation (*B*), and perpendicular (*C*) to the z-axis. All three scans were obtained with 1.0-pitch spiral technique and 2-mm-thick sections. *Arrow* marks vessel 1.

Fig 5. Example of beam-hardening artifact with the carotid phantom perpendicular to the z-axis (*A*). Note the bridging beam hardening across the stenosis (*arrow*). After MPR reconstruction, the artifacts are seen as black spots (*arrowhead*) at the expected locations of the vessels (*B*).

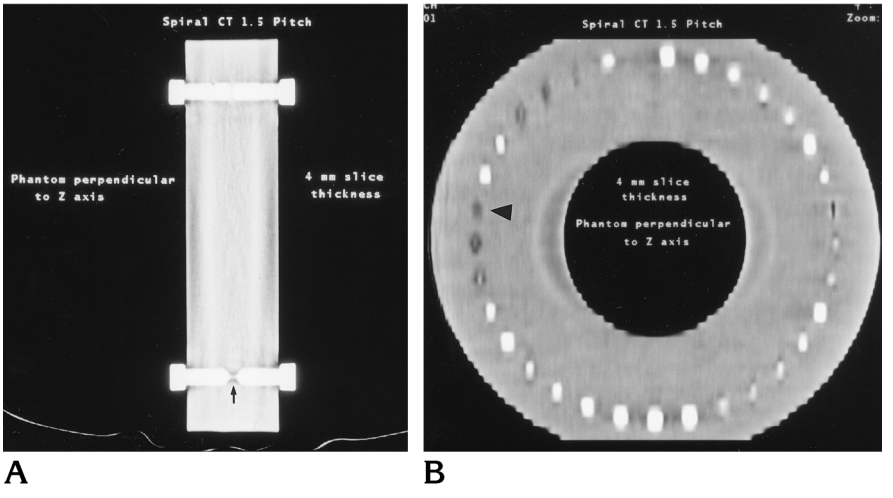

continuous data acquisition during peak contrast enhancement, which cannot be accomplished when using conventional CT.

Some studies have suggested that it is disadvantageous to perform CT angiography with higher pitch (1.5 to 2.0) spiral CT (7) (Diederichs et al, "Influence of Collimation..."). Other researchers have not found a significant detriment to using spiral CT with pitch greater than unity (6, 7). Our in vitro study verified these findings, demonstrating no significant increase in image artifacts or degradation in measurements of the percentage of stenosis with higher pitches.

Our results show that thinner sections and longer stenosis lengths improve the overall accuracy of CT angiography. The loss of accuracy with thicker images and shorter stenoses is most likely related to volume averaging of a normal-caliber vessel into the stenosis. Although other studies have reported that noise can be prohibitive when thin sections are used (6), significant image noise was not encountered in our study. The relatively high milliamperes and kilovolts (300 mA and 120 kV) used for the scans might account for this.

The vessel orientation relative to the z-axis also has importance for CT angiography. In our study, all three vessel orientations produced accurate results with longer stenoses and thinner sections, the 45° oblique vessel orientation being the least accurate of the three orientations and the orientation perpendicular to the z-axis the most accurate. However, image quality was significantly degraded with greater halo and edge artifacts in both the 45° oblique orientation and the orientation perpendicular to the z-axis. In addition, we found that artifactual occlusions

TABLE 5: Number of false occlusions relative to vessel orientation

Orientation	No. of False Occlusions
Parallel to Z-axis	0
45° Oblique	21
Perpendicular to Z-axis	58

with these two vessel orientations can significantly impair the assessment of high-grade stenoses in vessels not parallel to the z-axis. Therefore, the optimal CT angiographic assessment with the least amount of artifact is obtained with vessels parallel to the z-axis.

In addition to the effect of vessel orientation, both halo and edge artifacts are worse in conjunction with stenoses and directly correlate with the degree of luminal narrowing. Such artifacts were encountered less frequently in conventional CT studies when using thin sections and when vessels were oriented parallel to the z-axis. Although the degree of halo artifact may be related to the density of contrast in the vessel, this relationship was not evaluated and additional studies would be necessary to define its relationship to luminal enhancement.

We observed two interesting artifacts in relation to CT angiography. First, there was an eccentric luminal distortion on the 45° oblique MPR image and on the MPR image perpendicular to the z-axis. This distortion of round or spherical objects was described in the in vitro study by Kalender et al (10), and is related to broadening of the section sensitivity profile along the z-axis with resultant alignment of the halo and edge artifacts along the long axis of the lumens. The relatively focal display of artifact and luminal distortion in higher grade stenoses may contribute to the false occlusions seen with the 45° oblique vessel orientation and to a lesser extent with the perpendicular to the z-axis orientation. This disproportionate eccentricity in the stenoses may have significant implications, as measurements of stenoses that neglect this artifact may be adversely affected.

The second observed artifact was beam-hardening across stenoses in the perpendicular to the z-axis orientation. This artifact was the primary cause for the significant number of false occlusions identified in this vessel orientation and may actually be so severe as to produce apparent luminal discontinuity in high-grade stenoses. Such an artifact may in part explain the discrepant tendency of this study to underestimate stenoses relative to earlier clinical studies assessing renal artery stenoses (exclusively in the perpendicular to the z-axis orientation) that reported slight overestimation of stenoses with CT angiography (11).

The volume averaging effect combined with the very short stenosis lengths used in this study is the most likely explanation for the overall tendency to underestimate stenoses, which was particularly severe with the high-grade stenoses, short stenosis lengths, and greater section thicknesses. Conceivably, the choice of a window of 300 and level of 40 may have contributed to the underestimation of stenoses. However, the window and level settings used to measure stenoses were the same as those used to assess artifacts.

Does CT angiography reliably detect high-grade stenoses and occlusions? We identified 87 false occlusions out of 1152 vessels. However, there was one set of phantom vessels with a 1-mm long occlusion that was not detected on any of the scans. Although the clinical applicability of a 1-mm occlusion may be questioned, there is most likely a threshold occlusion length for detection by CT angiography.

Several aspects of our study deserve discussion. First, our phantom study was applied to only short stenoses (5 mm and less). The conclusions made from the study of these relatively short stenoses may or may not be applicable to the assessment of longer length stenoses. Second, vessels oriented parallel to the z-axis did not require MPR, whereas scans from the other two vessel orientations underwent MPR prior to luminal measurements and artifactual assessment. The oblique MPR required loading the primary CT scans onto a Picker Voxel Q workstation and then rotating the volume on the axis of the phantom to make the vessels parallel to the z-axis orientation. This additional yet necessary reconstruction undoubtedly contributed to the observed artifacts. Third, the results of this study were based on CT scans acquired on only one type of scanning system. The interpolation algorithms and MPR reconstruction methods vary among manufacturers, and the use of other systems may affect the reproducibility of these results.

Our observations and conclusions may have relevance to the clinical application of CT angiography, as clinical protocols require consideration of all imaging variables and factors inherent to the vessels of interest. Furthermore, the scanning parameters combined with the se-

verity and nature of vessel stenoses have an integrated impact on the quality and accuracy of CT angiographic assessment. Additional phantom and clinical studies are needed to address other variables, such as the role of section overlap and the effect of different contrast densities.

References

1. Dillon M, van Leeuwen M, Fernandez MA. Spiral CT angiography. *AJR Am J Roentgenol* 1993;160:1273–1278
2. Schwartz R, Jones K, Chernoff D, et al. Common carotid artery bifurcation: evaluation with spiral CT. *Radiology* 1992;185:513–519
3. Beauchamp N Jr. Spiral CT angiography: a new technique for evaluating the neurovasculature. *Appl Radiol* 1995;24(Suppl): 15–20
4. Park J, Chung J, Im J, et al. Takayasu arteritis: evaluation of mural changes in the aorta and pulmonary artery with CT angiography. *Radiology* 1995;196:89–93
5. Lawrence J, Kim D, Kent KC, et al. Lower extremity spiral CT angiography versus catheter angiography. *Radiology* 1995;194: 903–908
6. Brink J, Lim J, Wang G, et al. Technical optimization of spiral CT for depiction of renal artery stenosis: in vitro analysis. *Radiology* 1995;194:157–163
7. Rubin G, Napel S. Increased scan pitch for vascular and thoracic spiral CT. *Radiology* 1995;197:316–317
8. Cumming MJ, Morrow IM. Carotid artery stenosis: a prospective comparison of CT angiography and conventional angiography. *AJR Am J Roentgenol* 1994;163:517–523
9. Castillo M, Wilson JD. CT angiography of the common carotid artery bifurcation: comparison between two techniques and conventional angiography. *Neuroradiology* 1994;36:602–604
10. Kalender W, Polacin A, Suss C. A comparison of conventional and spiral CT: an experimental study on the detection of spherical lesions. *J Comput Assist Tomogr* 1994;18:167–176
11. Rubin G, Dake M, Napel S, et al. Spiral CT of renal artery stenosis: comparison of three-dimensional rendering techniques. *Radiology* 1994;190:181–189